ORIGINAL CONTRIBUTION

Clinical Trials of MR Thermography for Laser Ablation of Brain Tumors

Kagayaki KURODA[1,2,3], Joachim KETTENBACH[1,4], Arya NAVABI[1,5], Stuart G. SILVERMAN[1], Paul R. MORRISON[1], Ferenc A. JOLESZ[1]

[1]*Department of Radiology, Brigham and Women's Hospital, Harvard Medical School, Boston, MA, USA*
[2]*Department of Human and Information Sciences, Tokai University, Hiratsuka, Japan*
[3]*Department of Image-based Medicine, Institute of Biomedical Research and Innovation*
[4]*Department of Radiology, University Hospital of Vienna, Vienna, Austria*
[5]*Department of Neurosurgery, University of Kiel, Kiel, Germany*

The usefulness of MR temperature imaging in clinical practice is demonstrated here. Brain temperature changes under laser induced thermal therapy were imaged on a 0.5T open MR system in five patients with brain tumors. The phase mapping method was used. The images were obtained by a spoiled gradient echo sequence (TR/TE 50–55/14–34 ms; flip angle 20–30 degree; slice thickness 4–5 mm; FOV 320×240 or 300×300 mm; matrix 256×128). The resulting temperature maps clearly showed the temperature elevations, with a spatial and temporal resolution of 11–14 mm^3 and 7–8 s. The size of the hot regions were defined by contour plots with two different temperature coefficients (−0.01 and −0.00724 ppm/℃). These differed by only a few millimeters in diameter. This indicates that MR temperature images can demonstrate lesion size within an error range of a few millimeters even if the exact temperature coefficient for the patient's brain tissue is not known.

INTRODUCTION

Heat-based thermal therapies, such as laser-induced thermotherapy (LITT)[1),2)], focused ultrasound surgery (FUS)[3)], microwave (MW)[4)], and radio frequency (RF)[5)], are potentially useful, minimally invasive techniques to ablate tumor tissue. Compared with surgical resection, conventional radiotherapy and chemotherapy, these techniques are less invasive, do not require radiation, and generally result in damaging less normal tissue. LITT has been particularly useful for treating brain tumors[1),2)].

The key to a successful treatment is to position the laser fiber properly and to optimize the thermal dose to treat tumor tissue without damaging the surrounding normal tissues. To achieve this optimization, a practical and clinically useful non-invasive techniques for

Keywords temperature, chemical shift, phase mapping, brain, laser

MATERIALS AND METHODS

Table 1. Patient Data and Laser Parameters

Patient	Tumor location, type and diameter before treatment ［mm］	Sessions (all with a single fiber)	Power Setting ［W］	Radiation Duration ［sec］	Total Energy applied ［J］
1	Left frontal lobe High grade gliosarcoma 30×30	1	4	60	1440
		2	4	60	
		3 (5 mm withdrawn)	4	60	
		4 (further withdrawn)	4	60	
		5	4	60	
		6	4	60	
2	Left thalamic and hypothalamic Astrocytoma 25×20	1	2	60	960
		2 (withdrawn)	2	60	
		3	2	360	
3	Left fronto-parietal Glioma	1	2	288	576
4	Right frontal lobe Astrocytoma	1	5	120	3600
		2	5	300	
		3	5	300	
5	Left temporal lobe near midbrain and inferior thalamus Ganglioglioma	1	3	60	1086
		2	3	102	
		3	4	30	
		4	4	120	

55/14–34 ms ; flip angle, 20 –30° ; slice thickness, 4 –5 mm ; FOV, 320×240 or 300×300 mm ; matrix, 256×128 ; number of acquisitions, 1)[8),21)]. Imaging was initiated 30 s before each laser irradiation to obtain a baseline image, followed by continuous imaging until the end of each session. Then another set of images was obtained to monitor the cool-down period.

For on-line monitoring, all sequentially acquired images were transferred from the image buffer of the MR console to a research workstation (Sparc 20 TZX, Sun Microsystems, Inc., CA, USA) via the local network. An interactive graphical interface created by the authors' group was utilized to calculate and display color-coded temperature images on the workstation screen as well as the built-in-magnet liquid crystal display (LCD, Model LQ6NC01, Sharp Eletronics, Rahwah, NJ, USA). The temperature coefficient used for the on-line calculation was −0.01 ppm/℃. A detailed description of the on-line calculation can be found elsewhere [18,19)].

Off-line analysis was performed on a UNIX workstation (Macintosh G3/Mac OS X server, Apple Computer Inc., Cupertino, CA, USA) using plain C language and on a personal computer (Dimension XPS R450, Dell Computer Corp., TX, USA) using technical computing software (Matlab 5.2.0, The MathWorks Inc., MA, USA) to further examine the temperature imaging method and its characteristics. In this off-line examination, a temperature coefficient of −0.00724 ppm/℃, which was obtained in

mouse brain tissue in *vitro*[6], was also used. To compensate the phase change due to fluctuation or unexpected change in the external magnetic field, an average of the phase differences (between the baseline and the objective images) in four ROI's (each with 10×10 voxels) in the

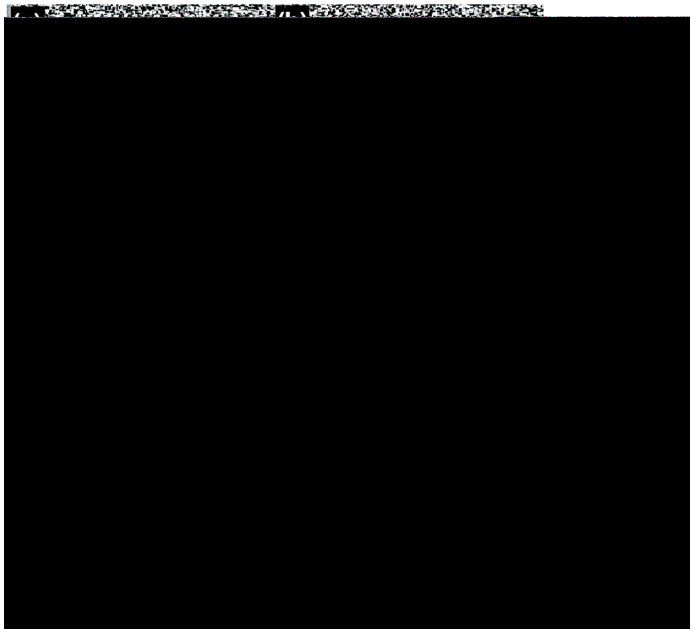

Fig. 1. Phase error induced by the change in the external magnetic field. The non-compensated phase differences (from the reference data) are displayed as the image intensities in (a) immediately after the laser was turned on and (b) 5 min later in session 3 for patient 2. There was a significant change in the phase difference between (a) and (b) over the non-heated regions. The change was approximately 0.2 ppm in the average in the ROI's (squares) which are distant from but surrounding the laser point (arrow). The phase change was well compensated in (c) and (d) by deducing the average phase change in the ROI's. The phase values in (c) and (d) became close to zero.

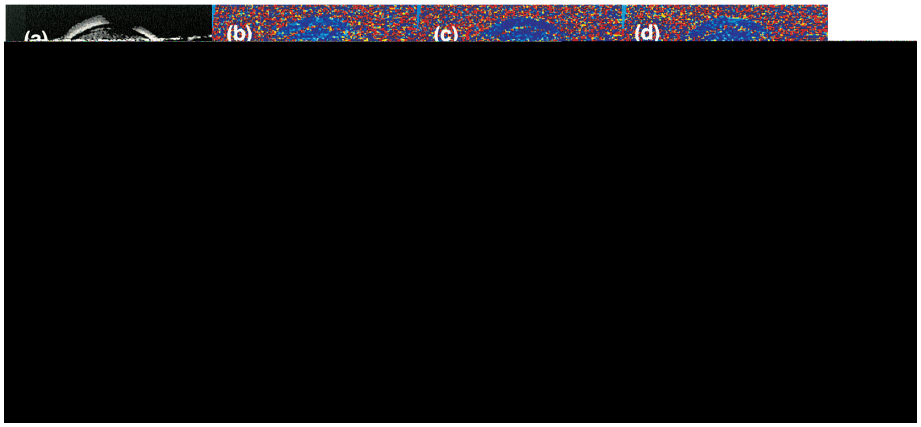

Fig. 2. Coronally oriented temperature elevation images of whole brain during a 6–minute laser irradiation (session 3) for patient 2. (a) T_1-weighted contrast-enhanced fast-spin echo image showing the target tumor with the laser fiber. (b) Immediately after the laser was turned on. (c) 1 min, (d) 2 min, (e) 3 min, (f) 4 min, (g) 5 min, and (h) 6 min later. The white strip on (b) is the region used to calculate the temperature profile shown in Fig. 4.

non-heated area away from but surrounding the laser tip was calculated and deducted from the entire slice plane.

RESULTS

Localization of tumor tissue, targeting, frameless stereotactic biopsy, and placement of the laser fiber were successfully performed by means of interactive image guidance[18)～20)] within the open configuration MR system. Since the treatment protocol was not optimized specifically for the temperature imaging sequences, three cases out of the five gave successful temperature imaging results.

Significant phase changes in the non-heated region were observed in all the three cases. A typical example (for patient 2) is shown in Fig. 1(a) and (b). The phase changes were as large as 0.2 ppm, which corresponded to 20℃ of temperature change. The erroneous changes in phase were effectively compensated by deducting the average of the phase differences in the ROI's (depicted in (a)), as shown in (c) and (d). The phase compensation in the same manner was applied to all the cases analyzed.

Figure 2 shows examples of the temperature elevation maps for the low power, long duration (session 3 for #2), together with the location of the laser fiber in the tumor. Figure 3 shows the contour plots of temperature elevation

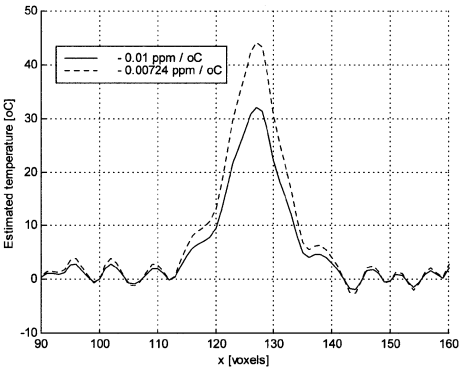

Fig. 4. Profile of the maximum temperature elevation (6 min after the laser was turned on) along the strip depicted in Fig. 2(b).

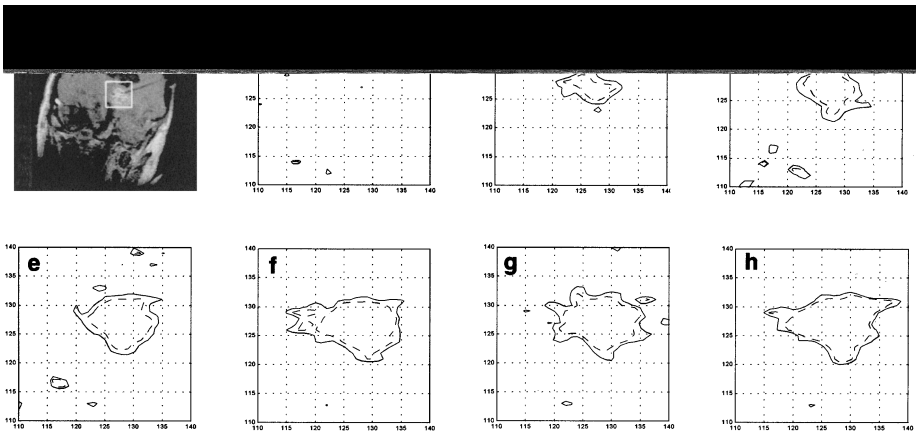

Fig. 3. Contour plots (within a square ROI shown in (a)) of 20℃ temperature elevation corresponding to the time course shown in (b) through (h) in Fig. 2. The solid contour was obtained based on the temperature coefficient of −0.00724 ppm/℃, while the dashed contour was based on −0.01 ppm/℃.

around the laser point estimated with different temperature coefficients. Figure 4 shows the profile of the temperature elevations along the strip depicted in Fig. 2(b).

DISCUSSION

We demonstrated the feasibility and usefulness of MR-based temperature imaging using a quantitative water proton chemical shift measurement during laser ablations for brain tumors. The results show that MR can be used to monitor transient thermal effects including heat loss in blood vessels. Conventional treatment was performed with temperature information obtained at the laser tip only, or based on the clinician's experience without a quantitative temperature measurement. Indeed, experienced surgeons may be skillful enough to perform LITT and to cover the entire tumor volume without measuring temperature, but it would be safer to use a quantitative temperature visualization technique. The phase mapping method of MR temperature imaging has been widely examined and its viability has been well established. Therefore the clinical experience of the method shown here was clearly necessary. In this study, we have focused on how the phase mapping method quantitatively depicts the temperature change and how much error could be estimated in a patient's brain. We visualized the temperature elevation in the brain lesion with a spatial and temporal resolution of 11 14 mm^3 and 7 8 s respectively. The LITT protocol differed patient by patient because of the process of our treatment invention. MR imaging indicated positions, sizes, and shapes of the heated regions, and approximate temperature elevation values at those various treatment procedures. These images also revealed that the temperature distribution induced by the laser was irregular-shaped as shown in Fig. 3. Since the process to create these images can be readily implemented as an online procedure, an operator should be able to compare the size of a high temperature region with the tumor size, and to control the laser power.

The temperature coefficient for the human brain is not known yet. One report in the literature evaluated the calibration of the water proton chemical shift measured with an NAA (N-Acetyl Aspartate) signal as an internal reference in an MRS volume in the human brain[22]. Tympanic membrane temperature, however, was used as a substitute for brain tissue temperature, and therefore the calibration was not direct. Although there have been several reports on the temperature coefficient in animal brains *in vivo*[13),22),23)] and *in vitro*[6),14)], the results are not consistent. This indicates that the temperature coefficients could vary according to tissue conditions, heating protocols, and animal species. Systematic calibration of the MR parameter[21)] in the *in vivo* brain and construction of the database for the temperature coefficient is required. However, it is not practical to place an invasive temperature probe (like an optical fiber thermometer or a thermocouple) in a patient's body. This fact makes a limit of the MR temperature imaging technique, because the temperature error has not been clear yet.

We examined the expected error in temperature estimation due to difference in the temperature coefficient without performing the calibration by putting an interstitial or a superficial temperature probe. The temperature elevation distributions in Fig. 2 were obtained using the temperature coefficient of -0.01 ppm/℃,

which is that of pure water[9]. The temperature elevation can be estimated 38% higher when the coefficient for mouse brain tissue *in vitro* (−0.00724 ppm/℃) is used (Fig. 4). This remarkable difference directly affects the maximum temperature estimation. However, as shown in the contour plots in Fig. 3, the hot spot sizes defined by a certain threshold (20℃), estimated with the different coefficients, differed only by a few millimeters in diameter. This indicates that the temperature images could indicate the lesion size within an error range of a few millimeters even if an exact temperature coefficient for the patient's brain tissue is not known.

When using the phase mapping method, the inter-image phase subtraction process is not significantly spoiled by motion when applied to the brain, which is stable when the head is firmly supported. However, the changes in blood volume and the oxygenation level of the red blood cells may change tissue susceptibility. The susceptibility change by a brain functional activation reaches as much as 0.05 ppm[24], which corresponds to 5℃ of temperature change. The susceptibility effects may be sufficiently reduced by using a spectroscopic imaging method[7),25] with NAA[22),23] as an internal reference to measure the water proton chemical shift.

A temperature-image-based, automated feedback system for the laser power control should be developed to improve treatment quality and accuracy, and to reduce the clinician's task load. The key to a practical system is that the hot region is outlined with a specific width related to a range of expected temperature coefficients (as the above-mentioned threshold contour plot) and that the growth of the region is compared with the outline of the tumor. Once the edge of the region hits the tumor, the laser power can be reduced or turned off. Development of a high-speed spectroscopic imaging method with internal reference[25] and an accurate calibration study would be important for future study.

CONCLUSIONS

The clinical feasibility of using MR-based temperature imaging for laser ablation using the phase mapping method was demonstrated. The resultant temperature elevation maps successfully indicated the position, size, shape, and temperature elevation value of the heated region. Although the analysis shown here was performed offline and its result was not directly used for the treatment control, those procedures could be easily transferred into online, real-time processing.

ACKNOWLEDGMENTS

The authors thank the members of the MRT clinical team of The Department of Radiology, Brigham and Women's Hospital for their effort in the clinical trials. This work was supported in part by grants from the National Institutes of Health (R01 CA 46627–08), National Science Foundation and GE Medical Systems. K. K. was supported by grants from the ministry of Education, Sciences and Culture of Japan, 11694172, Shimadzu Science Foundation of Japan, #10, and Nakatani Electronic Measuring Technology Association, #4. J. K. was supported by the Austrian Science Foundation and a Research and Education Fund of the European Congress of Radiology.

Authors are grateful fot that parts of this

work had received the International Exchange Grant and Award, Japan Society of Magnetic Resonance in Medicine, in 1999.

REFERENCES

1) Jolesz FA, Bleier AR, Jakab P, Ruenzel PW, Huttl K, Jako GJ : MR imaging of laser-tissue interactions. Radiology 1988 ; 168 : 249–253
2) Kahn T, Harth T, Kiwit JCW, Schawarzmaier H-J, Wald C, Mödder U : *In vivo* MRI thermometry using a phase-sensitive sequence : preliminary experience during MRI-guided laser-induced interstitial thermotherapy of brain tumors. J Magn Reson Imag 1998 ; 8 : 160–164
3) Cline HE, Hynynen K, Schneider E, Hardy CJ, Maier SE, Watkins RD, Jolesz FA : Simultaneous magnetic resonance phase and magnitude temperature maps in muscle. Magn Reson Med 1996 ; 35 : 309–315
4) Dodd GD 3rd, Soulen MC, Kane RA, Livraghi T, Lees WR, Yamashita Y, Gillams AR, Karahan OI, Rhim H : Minimally invasive treatment of malignant hepatic tumors : at the threshold of a major breakthrough. Radiographics 2000 ; 20 : 9–27
5) Goldberg SN, Gazelle GS, Muller PR : Thermal ablation therapy for focal malignancy : a unified approach to underlying principles, techniques, and diagnostic imaging guidance. AJR 2000 ; 174 : 323–331
6) Kuroda K, Abe K, Tsutsumi S, Ishihara Y, Suzuki Y, Satoh K : Water proton magnetic resonance spectroscopic imaging. Biomed Thermol 1994 ; 13 : 43–62
7) Kuroda K, Suzuki Y, Ishihara Y, Okamoto K, Suzuki Y : Temperature mapping by water proton chemical shift obtained with 3D-MRSI—Feasibility *in vivo*—. Magn Reson Med 1996 ; 35 : 20–29
8) Ishihara Y, Calderon A, Watanabe H, Okamoto K, Suzuki Y, Kuroda K, Suzuki Y : A precise and fast temperature mapping using water proton chemical shift. Magn Reson Med 1995 ; 34 : 814–823
9) Hindman JC : Proton resonance shift of water in gas and liquid states. J Chem Phy 1966 ; 44 : 4582–4592
10) Poorter JDe : Non-invasive MRI thermometry with the proton resonance frequency method : study of susceptibility effects. Magn Reson Med 1995 ; 34 : 359–367
11) Poorter JDe, Wagter Cde, Deene De, Thomsen C, Stahlberg F, Achten E : Non-invasive MRI thermometry with the proton resonance frequency shift (PRF) method : *in vivo* results in human muscle. Magn Reson Med 1995 ; 33 : 74–81
12) Young IR, Hajnal JV, Roberts IG, Ling JX, Hill-Cottingham RJ, Oatridge A, Wilson JA : An evaluation of the effects of susceptibility change on water chemical shift method of temperature measurement in human peripheral muscle. Magn Reson Med 1996 ; 36 : 366–374
13) Macfall JR, Prescott DM, Charles HC, Samulski TV : ^{1}H MRI phase thermometry *in vivo* in canine brain, muscle and tumor tissue. Med Phys 1996 ; 23 : 1775–1782
14) Peter RD, Hinks RS, Henkelman RM : *Ex vivo* tissue-type independence in proton-resonance frequency shift MR thermometry. Magn Reson Med 1998 ; 40 : 454–459
15) Moriaty JA, Chen JC, Purcell CM, et al. : MRI monitoring of interstitial microwave-induced heating and thermal lesions in rabbit brain *in vivo*. J Magn Reson Imag 1998 ; 8 : 128–135
16) Stollberger R, Huber D, Renhard W, Glanzer H : Influence of the temperature dependent susceptibility on monitoring of interstitial tissue coagulation using the proton resonance frequency method. Proc 5th ISMRM Meeting, Vancouver 1997 ; 3 : 1963
17) de Zwart JA, Vimeux FC, Delalande C, Moonen CTW : Fast lipid suppressed temperature mapping for the monitoring of focused ultrasound heated tissue. Proc 6th ISMRM Meeting, Sydney 1998 ; 1 : 350
18) Kettenbach J, Silverman SG, Hata N, et al. : Monitoring and visualization technique for MR-guided laser ablation in an open MR system. J Magn Reson Imag 1998 ; 8 : 933–943
19) Kettenbach J, Kuroda K, Hata N, et al. : Laser-

□□□□□□□ □□□□□□□□□□□□ □□ □□□□□□□□□ □□□□□□□□□ □□□ □□□ □□□□□□□□□□□□ □□□□□□□□ □□ □□□□□ □□□□ □ □□□□□□ □□□□□□□ □□□□ □ □/□ □ □□□–□□□

□□) □□□□□ □ □□ □ □□□□□□□□ □□ □□□□□□□□□□ □ □□□□ □□ □□□ □ □□□□□□□□□□□□□ □□□ □□□□□□□□□□□□□□ □□ □□□□□□□□□□□□ □□□□ □□□□□□□□ □□□□□□□□□ □□□□□□ □□□ □□□ □□□□ □□□□□□□□□□ □□□□□□□□□□□□□ □□□□□□□□□□□□□ □□□□ □ □□ □ □□□–□□□

□□) □□□□□□ □□ □□□□□ □□□ □□□□□□□□ □□ □□□□□□ □□ □ □□□□□□□□□□ □□ □□□□□ □□□□□□ □□□□□□□□ □□□□□□□□□□□□ □□□ □□□□□□□□□□□□ □□□□□□□□□□□ □□□□□ □□□ □□□□□□ □□□□□□□ □□□□□□□□□□ □□□□□□□□□ □ □□□□ □□□□□□ □□□□ □ □ □ □□□–□□□

□□) □□□□ □□□ □□□□□□□ □□□ □□□□□□□ □□ □□□ □ □ □□□ □□□□□□□□□□□ □□ □□□□□ □□□□□ □□□□□□□□□□□□ □□ *in vivo* □□ □□□□□□□□ □□□□□□□□□ □□□□□□□□□□□□□ □□□□ □□□□□ □ □□ □□□□ □ □□ □ □□□–□□□

□□) □□□□□□□ □□□□ □□□□□□□ □□□ □□□□□□□□□□ □□ □□□ □ □ □□□□ □□□□□□□□□□□□□ □□ □ □□□□□□□□□□□□ □□□□□□ □□ □□□□□□□□ □□□□□□□□□□□□ *in vivo* □□□□□ □□ □ □ □ □□□□□□□□□□□□□□□□□□□□ □□□□□□□□□□ □ □□□□ □ □□ □ □□□□–□□□□

□□) □□□□□□ □□ □□□□ □□ □□□□□ □□□ □□□□□□ □□ □□□□□ □ □ □□□□ □□□□□□□□□□□□□□□□□□□□ □□□□□□□□ □□ □□□□□□□□ □□□□□ □□□□□ □□□□□ □□□□□□□□ □□□□□ □□□□ □□□□□ □□□ □□□□ □ □□ □ □□–□□

□□) □□□□□□ □□ □□□□□ □□ □□□□□□ □□□ □□□□□□ □□□ □□□□□ □□ □ □□□□□ □□ □□□□□ □□ □□□□□□□□ □□ □□□□□□ □□ □ □□□□□□□□□□□ □□□□□□□ □□□□□ □□□□□ □□□□□ □□□□□□ □□□□ □□□□□□ □□□□□□□□□□□□□ □□□□□□□ □□□□ □□□□□ □□□□□□ □□□□□ □□ □□□□ □ □□ □ □□□–□□□